Optimized packing soft 3D polyhedra

Romanova Tetyana[a,b,c], Litvinchev Igor[d,*], Bennell Julia[a], Melashenko Oksana[b,e], Kravchenko Oleg[b] and Pankratov Olexandr[f]

[a]*Leeds University Business School, University of Leeds, Maurice Keyworth Building, Leeds, LS2 9JT, UK*
[b]*A. Pidgorny Institute of Power Machines and Systems of the National Academy of Sciences of Ukraine, Komunalnykiv, 2/10, Kharkiv, 61046, Ukraine*
[c]*Faculty of Computer Science, Kharkiv National University of Radio Electronics, Nauky Ave. 14, Kharkiv, 61166, Ukraine*
[d]*Faculty of Mechanical and Electrical Engineering, Autonomous University of Nuevo Leon, Pedro de Alba S/N, Niños Héroes, Ciudad Universitaria, Monterrey, 66455, Mexico*
[e]*Institute of Computer Sciences and Artificial Intelligence, V.N. Karazin Kharkiv National University, 4 Svobody Sq., Kharkiv, 61022, Ukraine*
[f]*Institute of Numerical Mathematics, Faculty of Mathematics, Technische Universität Dresden, Helmholtzstr. 10, Dresden, 01069, Germany*
E-mail: igor.litvinchev@uanl.edu.mx [I. Litvinchev]; tetiana.romanova@nure.ua, t.romanova@leeds.ac.uk [T. Romanova]; j.bennell@leeds.ac.uk [J. Bennell]; oksana.melashenko@karazin.ua [O. Melashenko]; krav@ipmach.kharkov.ua [O. Kravchenko]; oleksandr.pankratov@tu-dresden.de [O. Pankratov]

Abstract

A novel problem of packing soft convex 3D polyhedral objects in an optimized convex container is introduced. Soft objects can change their shapes within certain limits to better fit into the container, while preserving their volumes. Adjusted non-overlapping and containment conditions considering shape changes of soft objects are presented. Novel geometric tools are constructed to state explicitly these packing constraints, using the phi-function technique. The corresponding large-scale nonlinear nonconvex mathematical programming problem is introduced. To cope with high dimensionality a decomposition-based multistart heuristic is proposed. Numerical results are presented for packing soft tetrahedra and dodecahedra in minimum-volume cuboidal, spherical and cylindrical containers for different deformation parameters of objects. Based on real petrophysical data, a case study of digital core design is reported. The proposed approach is used for modeling porosity and particles shapes changes under external pressure. It is demonstrated that structural characteristics of the digital and natural cores are very similar.

Keywords: 3D packing; soft polyhedra; phi-function technique; mathematical modeling; nonlinear optimization; decomposition-based heuristic

1. Introduction

Optimized packing problems aim at allocating geometric objects completely within one or several containers without overlap, while minimizing either a metric characteristic (such as size, area, or volume) of the container or the number of containers used (see, e.g.,Wäscher et al. (2007); Oliveira et al. (2023); Chen et al. (2025); Hadj Salem et al. (2023)). In these settings, the shape of the container may be adjusted within certain limits, while the shapes of the objects are typically assumed to be fixed. Packing problems

*Author to whom all correspondence should be addressed (e-mail: igor.litvinchev@uanl.edu.mx).

of this type arise in logistics (Du et al. (2024)), 3D printing (Kim et al. (2024)), project management (Zhang (2004); Fasano (2014)), thermal deburring, space engineering (Fasano and Pintér (2016)), and raw material cutting (Fischer and Scheithauer (2015)), to mention only a few. In some variants, such as in the construction of convex hulls of geometric objects (Kallrath et al. (2021)), the shape of the container is not predefined and is determined through optimization. Packing problems for fixed-shape geometric objects are formulated and solved for various classes of regular (see, e.g., Scheithauer (2018); Romanova et al. (2020)) and irregular (see, e.g., Fasano (2014); Araújo et al. (2018); Leao et al. (2020); Chehrazad et al. (2025); Alvarez-Valdés et al. (2025)) 2D&3D shapes.

However, practical applications require arranging objects that can change their shapes to better fit the container. Typically, it is assumed that the volumes of objects remain constant under such shape changes. Depending on the application, these objects are referred to as compressible (Moghaddam and Baaj (2018)), deformable (Zuo et al. (2022); Coutinho et al. (2023)), elastic (Ma et al. (2023)), or soft (Murata and Kuh (1998)) objects. In the following, we use the term "soft objects".

Packing problems involving soft objects arise in floor planning (Ji et al. (2017)), logistics (Coutinho et al. (2023)), mechanics (Yuan et al. (2019)), biology (Jiang et al. (2019)), material science (Chen et al. (2021); Gou et al. (2020)), and nanotechnology (Winkelmann and Chan (2023)). The use of triangles or tetrahedra for mesh generation in finite element analysis can also be interpreted as a packing problem for soft objects (see, e.g., Lewis and Robinson (1978); Radovitzky and Ortiz (2000); Alliez et al. (2005); Conway and Torquato (2006)). In project management models (Hartmann (2000); Fasano (2014)), soft objects represent projects with fixed total resource consumption but flexible time schedules.

In the 2D case, various mathematical models and solution techniques are known for optimized packing of soft rectangles (see, e.g., Melashenko et al. (2025) and references therein), ellipses (Romanova et al. (2023)), and convex polygons (Bennell et al. (2024); Litvinchev et al. (2024b)). In the 3D case, a comprehensive study of packing soft spheres in a cylinder is presented in Winkelmann and Chan (2023), with applications to nanotechnology. The discrete element method combined with simulation approaches is typically used for packing basic 3D objects such as tetrahedra and cuboids (see, e.g., Zhao et al. (2020a,b); Qian and Li (2024) and references therein). To the best of our knowledge, packing soft convex 3D polyhedra has not been considered previously.

Our interest in packing soft 3D polyhedra is motivated by digital core reconstruction (see, e.g., Zhang et al. (2021); Ponomarev et al. (2022) and references therein). A core (a cylindrical rock sample extracted from subterranean formations) is originally located under relatively stable conditions, subject to high underground temperature and pressure. After extraction, the core is exposed to altered environmental conditions and gradually loses its original physical and chemical properties.

Core digitalization is a widely used method to address these issues, since core information can be reused without loss of microstructural properties, thereby reducing experimental costs. Digital cores aim to describe the microstructure of cores at the particle level and provide an effective way of analyzing pore structures and related properties in rock physics and petroleum science.

In mathematical models of digital cores, it is necessary to consider the effects of stress on particle shapes as well as particle size distributions. In contrast to the discrete element approach frequently used to address these issues (see, e.g., Wang et al. (2024) and references therein), we use an optimized packing model.

In this paper, packing of freely translated and rotated soft convex polyhedra in an optimized convex container is considered. Non-overlapping and containment conditions are formulated using the phi-

function approach (see, e.g., Chernov et al. (2010)). A special class of shape transformations, called "deformation", is introduced to represent shape changes under pressure. This transformation preserves the volume and convexity of a soft polyhedron.

The optimized packing problem is formulated as a nonlinear, nonconvex mathematical programming problem. Due to pairwise non-overlapping constraints, the number of variables and constraints grows quadratically with the number of objects (particles). A multistart decomposition-based heuristic is proposed to obtain efficient approximate solutions for large-scale problem instances. This approach is applied to modeling the granular structure and porosity of natural cores. Deformation of particle shapes enables the representation of granular matter behavior under external pressure.

The main contributions of this paper are as follows:

- A novel problem of packing freely translated and rotated soft convex 3D polyhedra in an optimized convex container is introduced.
- New non-overlapping, containment, and volume-preserving conditions are presented, considering shape changes of the objects.
- A corresponding nonlinear mathematical programming model is formulated.
- A decomposition-based heuristic is proposed to obtain efficient solutions for large-scale nonconvex optimization problems.
- Numerical experiments are provided to demonstrate the efficiency of the proposed approach.
- A case study of digital core design is presented, showing good agreement between experimental and modeling results.

The rest of the paper is organized as follows. Section 2 provides the basic mathematical constructions using the phi-function technique extended to soft polyhedra. The main nonlinear mathematical programming model for optimized packing of soft convex polyhedra is formulated. A decomposition-based multistart solution algorithm is stated in Section 3. Results of numerical experiments are presented in Section 4. A case study on digital core reconstruction in the oil industry is reported and discussed in Section 5, while Section 6 concludes the paper. Basic definitions related to the phi-function technique are summarized in Appendix A, while Appendix B provides a table of notations used in the paper.

2. Basic constructions and a mathematical model

Let P_i, $i \in I_n = \{1, 2, ..., n\}$ be a set of convex polyhedra (objects). Each polyhedron P_i is defined as the convex hull of a collection of its vertices $\tilde{X}_i^k = (\tilde{x}_i^k, \tilde{y}_i^k, \tilde{z}_i^k)$, $k \in J_i = \{1, 2, ..., m_i\}$, $i \in I_n$. Denote by $\Omega(L) \subset \mathbb{R}^3$ a convex bounded region (container) defined by a vector of its variable metric characteristics $L \in \mathbb{R}^\sigma, \sigma$ – is the number of variable metric characteristics of Ω.

Each polyhedron P_i can be rotated by angles $\theta_i^1, \theta_i^2, \theta_i^3$ and translated by a 3D vector v_i. The polyhedron can also be deformed along the axes Ox, Oy, Oz with bounded deformation parameters $(\mu_i^x, \mu_i^y, \mu_i^z)$, $\mu_x^- \le \mu_i^x \le \mu_x^+$, $\mu_y^- \le \mu_i^y \le \mu_y^+$, $\mu_z^- \le \mu_i^z \le \mu_z^+$ respectively. Here, low and upper bounds for deformation parameters are known non-negative constants. The corresponding transformed polyhedron is presented as

$$P_i(u_i, \mu_i) = \{p \in \mathbb{R}^3 : p = v_i + M(\theta_i) \cdot A(\mu_i) \cdot p^{0T}, \forall p^0 \in P_i^0\},$$

where $u_i = (v_i, \theta_i)$, $v_i = (x_i, y_i, z_i)$, $\theta_i = (\theta_i^1, \theta_i^2, \theta_i^3)$, $\mu_i = (\mu_i^x, \mu_i^y, \mu_i^z)$.

Here P_i^0 denotes the original non-translated, non-rotated and non-deformed polyhedron ($x_i = 0, y_i = 0, z_i = 0, \theta_i^1 = \theta_i^2 = \theta_i^3 = 0, \mu_i^x = \mu_i^y = \mu_i^z = 1$),

$A(\mu_i) = \begin{pmatrix} \mu_i^x & 0 & 0 \\ 0 & \mu_i^y & 0 \\ 0 & 0 & \mu_i^z \end{pmatrix}$ is the deformation matrix,

$M(\theta_i) = \begin{pmatrix} M_{11} & M_{12} & M_{13} \\ M_{21} & M_{22} & M_{23} \\ M_{31} & M_{32} & M_{33} \end{pmatrix}$ is the rotation matrix,

$$M_{11} = \cos\theta^2 \cos\theta^3, M_{12} = \cos\theta^3 \sin\theta^1 \sin\theta^2 - \cos\theta^1 \sin\theta^3,$$

$$M_{13} = \sin\theta^1 \sin\theta^3 + \cos\theta^1 \cos\theta^3 \sin\theta^2, M_{21} = \cos\theta^2 \sin\theta^3,$$

$$M_{22} = \cos\theta^1 cos\theta^3 + \sin\theta^1 \sin\theta^2 \sin\theta^3, M_{23} = \cos\theta^1 \sin\theta^2 \sin\theta^3 - \cos\theta^3 \sin\theta^1,$$

$$M_{31} = -\sin\theta^2, M_{32} = \cos\theta^2 \sin\theta^1, M_{33} = \cos\theta^1 \cos\theta^2.$$

Comment 1. Generally, a matrix product is not commutative, i.e., $M(\theta_i) \cdot A(\mu_i) \neq A(\mu_i) \cdot M(\theta_i)$. In the definition of the transformed polyhedron $P_i(u_i, \mu_i)$ above, deformation along principal axes is applied first, and then rotation is used. In this case the shape of the transformed polyhedron is similar to that of the original object. For example, if the original object P_i^0 is a cuboid (a rectangle in 2D), it will remain a cuboid (a rectangle) after the transformation $M(\theta_i) \cdot A(\mu_i)$. However, if rotation is applied first, and then deformation is used, the shape of the transformed object can be different after the transformation $A(\mu_i) \cdot M(\theta_i)$. For example, if the original object is a square, the transformed object may have a rhomboid shape.

Each vertex $\tilde{X}_i^k = (\tilde{x}_i^k, \tilde{y}_i^k, \tilde{z}_i^k)$ after rotating, translating and deforming the original polyhedron P_i^0 is denoted as $X_i^k = (x_i^k, y_i^k, z_i^k) \in \mathbb{R}^3$, were

$$\left.\begin{array}{l} x_i^k = (M_{11}\tilde{x}_i^k + M_{12}\tilde{y}_i^k + M_{13}\tilde{z}_i^k) \cdot \mu_i^x + x_i, \\ y_i^k = (M_{21}\tilde{x}_i^k + M_{22}\tilde{y}_i^k + M_{23}\tilde{z}_i^k) \cdot \mu_i^y + y_i, \\ z_i^k = (M_{31}\tilde{x}_i^k + M_{32}\tilde{y}_i^k + M_{33}\tilde{z}_i^k) \cdot \mu_i^z + z_i. \end{array}\right\} \quad (1)$$

Proposition 1. If

$$\mu_i^x \cdot \mu_i^y \cdot \mu_i^z = 1, \quad (2)$$

then the deformation transformation $A(\mu_i)$ preserves the volume and convexity of the polyhedron $P_i(u_i, \mu_i)$.

Demonstration. Let T be a square nonsingular $m \times m$ matrix with $\det T \neq 0$, while A be an $q \times m$ matrix, and $b \in \mathbb{R}^q$. Denote $S_x = \{x \in \mathbb{R}^m : Ax \leq b\}$ and assume that S_x is a bounded set in $\mathbb{R}^m$. Consider a linear transformation of variables $x = Ty$ and denote $S_y = \{y \in \mathbb{R}^m : ATy \leq b\}$. Since T is nonsingular, then S_y is also bounded. Using the formula for change in variables in multiple integral (see, e.g., Schwartz (1954)), we have

$$\int_{S_x} dx = |\det T| \int_{S_y} dy.$$

For $n = 3$ we have the following correspondence between volumes of the S_x, S_y: $vol(S_x) = |\det T| \cdot vol(S_y)$. In the case of deforming transformation, we have $T = diag\{\mu_i^x, \mu_i^y, \mu_i^z\}$ and $\det T = \mu_i^x \times \mu_i^y \times \mu_i^z$. Correspondingly, if $\mu_i^x \times \mu_i^y \times \mu_i^z = 1$, then a polyhedral object P_i^0 does not change its volume under the deformation. Also, if the convex polyhedral object P_i^0 is defined by a system of linear inequalities S_x, then the deformed object $P_i(u_i, \mu_i)$ is defined by the linear system S_y and thus is convex.

In what follows we will assume that deformation parameters fulfill the condition $\mu_i^x \cdot \mu_i^y \cdot \mu_i^z = 1$.

Figure 1 shows examples of the shape transformations of a soft regular dodecahedron $P_i(u_i, \mu_i)$ for different deformation parameters $\mu_i^x, \mu_i^y, \mu_i^z$ under the volume preservation.

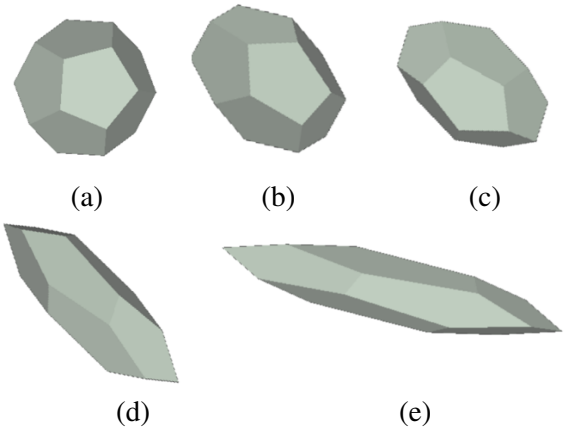


Fig. 1. Shapes of a soft polyhedron under its volume preservation for different deformation parameters: (a) $\mu_i^x = 1,\ \mu_i^y = 1,\ \mu_i^z = 1$; (b) $\mu_i^x = 0.64,\ \mu_i^y = 1.25,\ \mu_i^z = 1.25$; (c) $\mu_i^x = 1.44,\ \mu_i^y = 0.83,\ \mu_i^z = 0.83$; (d) $\mu_i^x = 2.25,\ \mu_i^y = 0.67,\ \mu_i^z = 0.67$; (e) $\mu_i^x = 3.0625,\ \mu_i^y = 0.57,\ \mu_i^z = 0.57$

A packing problem for soft polyhedra with variable deformation parameters is considered in the following form:

Find deformation parameters and a placement of soft polyhedra $P_i(u_i, \mu_i)$, $i \in I_n$, in a minimum-volume convex container $\Omega(L)$ under the following conditions:

- polyhedra do not overlap, but can be tangent (non-overlapping condition);
- polyhedra are placed completely inside the container (containment condition);
- polyhedra remains convex under deformation (convexity preservation);
- polyhedra do not change their volumes under deformation (volume preservation).

The non-overlapping condition, $intP_i(u_i, \mu_i) \bigcap intP_j(u_j, \mu_j) = \emptyset$, can be defined using the concept of quasi-phi-function (see Stoyan et al. (2016) and Appendix A for basic definitions).

Comparing to quasi-phi-functions for rigid polyhedra (Romanova et al. (2018)), the quasi-phi-function for soft polyhedra P_i and P_j used in this paper depends not only on their variable motion vectors u_i, u_j and separated plane coefficients τ_{ij}, but also on their variable vectors μ_i and μ_j of deformation parameters, fulfilling constraint (2).

Let $H(\tau_{ij}) = \{(x, y, z) :\ \alpha_{ij} \cdot x + \beta_{ij} \cdot y + \gamma_{ij} \cdot z + \delta_{ij} \geq 0\}$ be a half space with variable parameters $\tau_{ij} = (\theta_{ij}^x, \theta_{ij}^y, \delta_{ij}) \in \mathbb{R}^3$, $\alpha_{ij} = \sin\theta_{ij}^y$, $\beta_{ij} = -\sin\theta_{ij}^x \cdot \cos\theta_{ij}^y$, $\gamma_{ij} = \cos\theta_{ij}^x \cdot \cos\theta_{ij}^y$.

A quasi-phi-function for soft polyhedra $P_i(u_i, \mu_i)$ and $P_j(u_j, \mu_j)$ can be defined as follows:

$$\varphi_{ij}(u_i, u_j, \mu_i, \mu_j, \tau_{ij}) = \min\{\varphi^{P_i H}(u_i, \mu_i, \tau_{ij}), \varphi^{P_j H^*}(u_j, \mu_j, \tau_{ij})\},$$

where $\varphi^{P_i H}(u_i, \mu_i, \tau_{ij}) = \min\limits_{1 \le k \le m_i} (\alpha_{ij} \cdot x_i^k + \beta_{ij} \cdot y_i^k + \gamma_{ij} \cdot z_i^k + \delta_{ij})$ is the normalized phi-function for $P_i(u_i, \mu_i)$ and $H_{ij}(\tau_{ij})$, while

$\varphi^{P_j H^*}(u_j, \mu_j, \tau_{ij}) = \min\limits_{1 \le k \le m_j} (-\alpha_{ij} \cdot x_i^k - \beta_{ij} \cdot y_i^k - \gamma_{ij} \cdot z_i^k - \delta_{ij})$ is the normalized phi-function for $P_j(u_j, \mu_j)$ and $H_{ij}^*(\tau_{ij}) = \mathbb{R}^3 \backslash H_{ij}(\tau_{ij})$.

Note that $\max\limits_{\tau_{ij}} \Phi_{ij}(u_i, u_j, \tau_{ij}, \mu_i, \mu_j)$ is a phi-function for soft polyhedra $P_i(u_i, \mu_i)$ and $P_j(u_j, \mu_j)$. Hence, by the quasi-phi-function definition, the inequality $\Phi_{ij}(u_i, u_j, \mu_i, \mu_j, \tau_{ij}) \ge 0$ ensures the non-overlapping of soft polyhedra $P_i(u_i, \mu_i)$ and $P_j(u_j, \mu_j)$.

The containment condition $P_i(u_i, \mu_i) \subset \Omega(L) \Leftrightarrow intP_i(u_i, \mu_i) \bigcap \Omega^*(L) = \emptyset$, $\Omega^*(L) = \mathbb{R}^3 \backslash int\Omega(L)$, can be described as $\psi_i(u_i, \mu_i, L) \ge 0$.

Here $\psi_i(u_i, \mu_i, L)$ is a phi-function of the soft polyhedron $P_i(u_i, \mu_i)$ and the object $\Omega^*(L)$ (see Chernov et al. (2010) and Appendix A for basic definitions).

In comparison with the phi-function for a rigid polyhedron and the complement to a container (Romanova et al. (2018)), the phi-function for a soft polyhedron P_i and the object Ω^* depends not only on variable motion vector u_i of polyhedron P_i but also on its variable vector μ_i of deformation parameters, fulfilling constraint (2).

The coordinates of the vertices of the soft polyhedron are defined by formulas (1). Since all soft polyhedral objects and the container are convex, the containment condition in fact states that all vertices of the polyhedral objects are in the container. The expression of $\psi_i(u_i, \mu_i, L)$ depends on the shape of the container. In this paper we focus on three types of containers: a cuboid, a sphere and a cylinder.

If $\Omega(L = (a, b, c))$ is a cuboid, $\Omega = \{(x, y, z) : 0 \le x \le a, 0 \le y \le b, 0 \le z \le c\}$, then

$$\psi_i(u_i, \mu_i, a, b, c) = \min_{t=1,\dots,6} \psi_{it}(u_i, \mu_i, a, b, c),$$

where

$$\psi_{i1}(u_i, \mu_i, a, b, c) = x_i^k, \psi_{i2}(u_i, \mu_i, a, b, c) = -x_i^k + a,$$

$$\psi_{i3}(u_i, \mu_i, a, b, c) = y_i^k, \psi_{i4}(u_i, \mu_i, a, b, c) = -y_i^k + b,$$

$$\psi_{i5}(u_i, \mu_i, a, b, c) = z_i^k, \psi_{i6}(u_i, \mu_i, a, b, c) = -z_i^k + c.$$

If $\Omega(L = r)$ is a sphere, $\Omega = \left\{(x, y, z) : -x^2 - y^2 - z^2 + r^2 \ge 0\right\}$, then

$$\psi_i(u_i, \mu_i, r) = \min_{k \in J_i}(r^2 - (x_i^k)^2 - (y_i^k)^2 - (z_i^k)^2).$$

If $\Omega(L = (r, h))$ is a cylinder, $\Omega = \left\{(x, y, z) : -x^2 - y^2 + r^2 \ge 0,\ 0 \le z \le h\right\}$, then

$$\psi_i(u_i, \mu_i, r, h) = \min\{\min_{k \in J_i}(r^2 - (x_i^k)^2 - (y_i^k)^2), \min_{k \in J_i} z_i^k, \min_{k \in J_i}(-z_i^k + h)\},$$

where x_i^k, y_i^k, z_i^k are defined in (1).

A mathematical model for packing soft polyhedra can be represented as a nonlinear programming problem as follows:

$$\min_{u,\tau,\mu,L} \kappa(L) \tag{3}$$

subject to

$$\varphi_{ij}(u_i, u_j, \mu_i, \mu_j, \tau_{ij}) \geq 0, (i,j) \in \Lambda, \tag{4}$$

$$\psi_i(u_i, \mu_i, L) \geq 0, i \in I_n, \tag{5}$$

$$\mu_i^x \cdot \mu_i^y \cdot \mu_i^z = 1, i \in I_n, \tag{6}$$

$$\mu_x^- \leq \mu_i^x \leq \mu_x^+,\ \mu_y^- \leq \mu_i^y \leq \mu_y^+,\ \mu_z^- \leq \mu_i^z \leq \mu_z^+,\ i \in I_n, \tag{7}$$

where

$$u = (u_i, i \in I_n), u_i = (v_i, \theta_i), v_i = (x_i, y_i, z_i), \theta_i = (\theta_i^1, \theta_i^2, \theta_i^3), \tau = (\tau_{ij}, (i,j) \in \Lambda),$$

$$\tau_{ij} = (\phi_{ij}, \gamma_{ij}), \Lambda = \{(i,j) \in I_n \times I_n : i < j\}, \mu_i = (\mu_i^x, \mu_i^y, \mu_i^z), \mu = (\mu_i, i \in I_n).$$

The objective function $\kappa(L)$ characterizes the volume of the container and depends on its shape. For example, $\kappa(L = r) = r$ for a spherical container, $\kappa(L = (r,h)) = r^2 \cdot h$ for a cylindrical container, $\kappa(L = (a,b,c)) = a \cdot b \cdot c$ for a cuboidal container.

The problem (3)–(7) is a large-scale nonlinear nonconvex mathematical programming problem having $O(n^2)$ variables and constraints. It can be solved efficiently only for a relatively small number n of objects (see Section 3 for details).

In the next section a heuristic decomposition-based solution approach is proposed aimed at reducing the number of nonlinear non-overlapping constraints handled in each iteration.

3. A solution approach

To solve the problem (3)–(7), a multistart strategy is used, which includes three main stages. At the first stage, a set of feasible starting points is formed (see Algorithm 1 below). The second stage implements the search for local minima of the problem (3)–(7) for each starting point obtained at the first stage, using a decomposition approach (see Algorithm 2 below). At the third stage, the best solution obtained at the second stage is selected. This result is considered as a solution to the problem (3)–(7).

Algorithm 1. Constructing feasible starting points for packing 3D soft objects.

We define a circumscribed sphere $S_i(v_i)$ of radius r_i for each original polyhedron $P_i(u_i)$, $i \in I_n$. The key idea of the algorithm is based on homothetic transformations of spheres circumscribed around the original polyhedra. These scaling spheres grow inside a unit container as much as possible and then are scaled to original sizes providing a configuration of polyhedra feasible to problem (3)–(7).

Step 1. Generate a set of random points $v_i' = (x_i', y_i', z_i')$, $i \in I_n$, within a "unit" container Ω' (for example, a sphere of radius $r' = 1$; a cuboid of dimensions $a' = 1, b' = 1, c' = 1$; a cylinder of dimensions $r' = 1$, $h' = 1$. Define a vector $v' = (v_1', \ldots, v_n')$.

Step 2. Grow the spheres $\lambda S_i(v_i), i \in I_n$ within the "unit" container Ω' centered at $(0,0,0)$, solving the following nonlinear programming problem:

$$\max_{v,\lambda} \lambda \tag{8}$$

subject to

$$\omega_{ij}(v_i, v_j, \lambda) \geq 0,\ (i,j) \in \Lambda = \{(i,j) \in I_n \times I_n : i < j\}, \tag{9}$$

$$\omega_i(v_i, \lambda) \geq 0, i \in I_n, \tag{10}$$

$$0 \leq \lambda \leq 1, \tag{11}$$

starting from the point $(v', \lambda' = 0)$.

In problem (8)–(11), the variable λ is a scaling parameter of each sphere $S_i,\ i \in I_n$, $\omega_{ij}(v_i, v_j, \lambda)$ is the phi-function of $\lambda S_i(v_i)$ and $\lambda S_j(v_j)$ for $(i,j) \in \Lambda$, while $\omega_i(v_i, \lambda)$ is the phi-function of the objects $\lambda S_i(v_i)$ and $\bar{\Omega}' = \mathbb{R}^3 \backslash int S'$ for $i \in I_n$.

Note that inequalities (9) and (10) provide the conditions of non-overlapping and containment for the scaling spheres $\lambda S_i(v_i)$, $i \in I_n$, considering the constraint (11).

Denote a (local) solution to the problem (8)–(11) by (v'', λ'').

Step 3. Set $L^{(0)} = \frac{1}{\lambda''}$, $x_i^{(0)} = \frac{x_i''}{\lambda''}$, $y_i^{(0)} = \frac{y_i''}{\lambda''}$, $z_i^{(0)} = \frac{z_i''}{\lambda''}$.

Step 4. Define vector $u^{(0)} = (u_1^{(0)}, ..., u_n^{(0)})$,

where $u^{(0)} = (v^{(0)}, \theta^{(0)})$, $\theta^{(0)} = (\theta_1^{(0)}, ..., \theta_n^{(0)})$ is a vector of randomly chosen rotation angles $\theta_i^{(0)} = (\theta_i^{1(0)}, \theta_i^{2(0)}, \theta_i^{3(0)})$, $\theta_i^{1(0)} \in [0, 2\pi)$, $\theta_i^{2(0)} \in [0, 2\pi)$, $\theta_i^{3(0)} \in [0, 2\pi)$, $i \in I_n$, $\tau^{(0)} = (\tau_{ij}^{(0)}, (i,j) \in \Lambda)$, $\tau_{ij}^{(0)}$ is a vector of parameters of a separating plane for a pair of spheres $S_i(v_i^{(0)})$ and $S_j(v_j^{(0)})$, $(i,j) \in \Lambda$.

The point $(u^{(0)}, \tau^{(0)}, r^{(0)})$ is used as a feasible starting point to solve the problem (3)–(7).

Figure 2 illustrates principal steps of Algorithm 1 for the problem (8)–(11). Cases (a)-(e) correspond to Step 2 for different values of the scaling parameter λ: (a) $\lambda = 0.01$, (b) $\lambda = 0.03$, (c) $\lambda = 0.05$, (d) $\lambda = 0.1$, (e) $\lambda^* = 0.1329$, while cases (f)-(g) correspond to Step 3 and Step 4 of the Algorithm 1.

Thus, Algorithm 1 provides feasible starting points to the problem (3)–(7).

To search for local extrema of the problem (3)–(7), a decomposition technique is used. This approach reduces a large-scale problem (3)–(7) to a sequence of nonlinear programming problems of much lower dimension based on the idea proposed in (Romanova et al. (2020)) for fixed-shape objects.

Algorithm 2. Decomposition algorithm for 3D soft objects.

Our decomposition algorithm is an iterative procedure and involves the following steps.

Let $(u^{(0)}, \tau^{(0)}, \mu^{(0)})$, $u^{(0)} = (v^{(0)}, \theta^{(0)})$, $\tau^{(0)}$ be found by Algorithm 1 for $X^{(0)}$ and Ω^0.

Step 1. Set iteration number $t = 0$.

Step 2. Fix parameters $u_i^{(t)} = (v_i^{(t)}, \theta_i^{(t)})$, $i \in I_n$.

Step 3. Construct a cube $B_i^{(t)}$ with side $2(r_i + \delta)$ and centered at the point $v_i^{(t)}$, $i \in I_n$, $\delta = \mu^+ \cdot \max_{i \in I_n} r_i$, where r_i is the radius of the sphere $S_i(v_i)$ circumscribed around the original polyhedron $P_i(u_i)$.

Step 4. Fix $B_i^{(t)}$, $i \in I_n$.

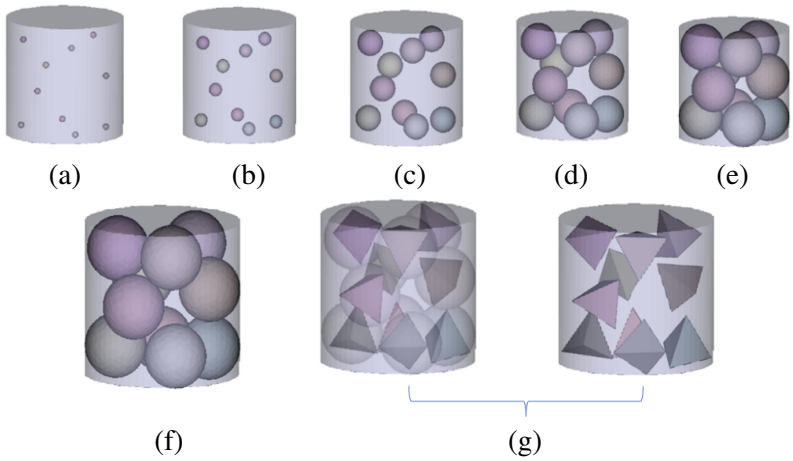


Fig. 2. Illustration of principal steps of the Algorithm 1.

Step 5. Set $t = t + 1$. Define a system of linear inequalities

$$x_i - x_i^{(t-1)} + \delta \geq 0, x_i^{(t-1)} - x_i + \delta \geq 0, y_i - y_i^{(t-1)} + \delta \geq 0, y_i^{(t-1)} - y_i + \delta \geq 0,$$

$$z_i - z_i^{(t-1)} + \delta \geq 0, z_i^{(t-1)} - z_i + \delta \geq 0,$$

denoted by $f^{(t)}(v_i) \geq 0,\ i \in I_n$.

Step 6. Solve the following nonlinear programming problem:

$$\min_{u,\tau,\mu} \kappa \tag{12}$$

subject to

$$\varphi_{ij}(u_i, u_j, \mu_i, \mu_j, \tau_{ij}) \geq 0,\ (i,j) \in \Lambda^{(t)}, \tag{13}$$

$$\psi_i(u_i, \mu_i) \geq 0,\ i \in I_n, \tag{14}$$

$$f^{(t)}(v_i) \geq 0,\ i \in I_n, \tag{15}$$

$$\mu_i^x \cdot \mu_i^y \cdot \mu_i^z = 1, i \in I_n, \tag{16}$$

$$\mu_x^- \leq \mu_i^x \leq \mu_x^+, \mu_y^- \leq \mu_i^y \leq \mu_y^+, \mu_z^- \leq \mu_i^z \leq \mu_z^+, i \in I_n, \tag{17}$$

where $\Lambda^{(t)} = \{(i,j) : B_i^{(t-1)} \cap B_j^{(t-1)} \neq \emptyset, i \in I_n, j \in I_n, i < j\}$.

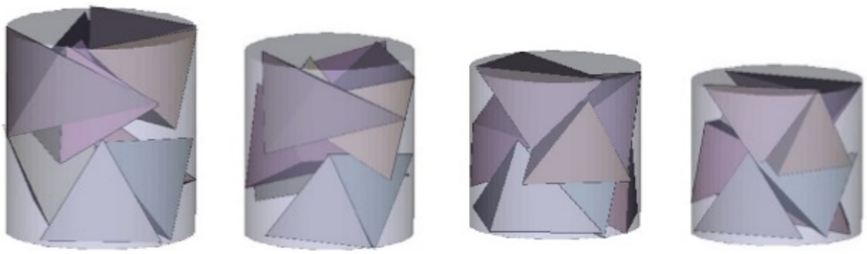
Step 7. If $\left|\kappa^{(t)} - \kappa^{(t-1)}\right| \leq \varepsilon$, then stop Algorithm 2, otherwise go to step 8.

Step 8. Take the point of the local minimum of the problem (12)–(16) as a feasible starting point and go to Step 2.

Instead of all pairs of polyhedra considered in non-overlapping constraints (4), Algorithm 2 typically involves much fewer pairs since for each polyhedron only its "δ-neighbors" must be analysed. Parameter

δ controls a balance between dimensions of subproblems (12)–(17) and the number of subproblems (12)–(17) to solve. The decomposition Algorithm 2 reduces the large-scale problem (3)–(7) to a sequence of subproblems (12)–(17) with a considerably smaller number of variables and constraints.

Figure 3(a) presents a feasible starting point found by Algorithm 1. Figures 3(b)-3(d) correspond to local minima of the problem (12)–(17) obtained at iterations $t = 1, 2, 3$. Figure 3 illustrates three iterations $t = 1, 2, 3$ of solving the problem (12)–(17) in step 6 of Algorithm 2. In this example, Algorithm 2 terminates at the third iteration (Step 7).



(a) (b) (c) (d)

Fig. 3. Three iterations of the decomposition algorithm at Step 6.

4. Computational experiments

This section presents experimental results for packing soft polyhedra. The choice of regular polyhedra (as original shapes) for experimentations is motivated by their frequent use in modelling various processes in natural sciences (see, e.g., Zhao et al. (2015); Xie et al. (2017); Zhao et al. (2020a,b); Guo et al. (2023); Dahle et al. (2023); Januszewski and Zielonka (2024); Lu et al. (2025)). Three types of containers are considered: cuboid $\Omega(L = (a, b, c))$, sphere $\Omega(L = (r))$ and cylinder $\Omega(L = (r, h))$. In each problem instance, three feasible starting points are used. In Tables 1–6 below, V^* denotes the volume of the optimized container, $f^* = (\sum_{i=1}^{n} V_i)/V^*$ is the container filling factor, where $V^*(sphere) = \frac{4}{3}\pi(r^*)^3$, $V^*(cuboid) = a^*b^*c^*$, $V^*(cylinder) = \pi h^*(r^*)^2$.

Denote the radius of a sphere circumscribed around a regular polyhedron as $r^{(i)}$. Then the volume V_i of a regular tetrahedron with the edge-length $a^{(i)} = 2r^{(i)}\sqrt{\frac{2}{3}}$ is expressed as $V^{(i)} = \frac{\sqrt{2}(a^{(i)})^3}{12}$ ($r^{(i)} = 3$), while the volume of a regular dodecahedron with the edge-length $a^{(i)} = \frac{4r^{(i)}}{(1+\sqrt{5})\sqrt{3}}$ is derived by $V^{(i)} = \frac{(15+7\sqrt{5})}{4}(a^{(i)})^3$ ($r^{(i)} = 2$) (see, e.g., Bronshtein et al. (2015)). Since in our model volumes of objects remain constant under shape transformations, these expressions define also volumes of the transformed objects.

Note, that though the bounds μ^-, μ^+ for the deformation parameters are just the same for all objects, optimal values of deformation parameters $\mu_i^x, \mu_i^y, \mu_i^z, i \in I_n$ are object-dependent. We consider two groups of instances both for tetrahedra and dodecahedra. In the first group of instances we set the tetrahedron variable deformation parameters $\mu_i^x = \bar{\mu}_i,\ \mu_i^y = 1/\bar{\mu}_i,\ \mu_i^z = 1$, for $i \in I_n$ (see Table 1 for

$\mu^- \le \bar{\mu}_i \le \mu^+$) and the dodecahedron variable deformation parameters $\mu_i^x = \bar{\mu}_i^2,\ \mu_i^y = 1/\bar{\mu}_i,\ \mu_i^z = 1/\bar{\mu}_i, \mu^- \le \bar{\mu}_i \le \mu^+$ for $i \in I_n$ (see Table 3 for $\mu^- \le \bar{\mu}_i \le \mu^+$). In both cases, a specific relationship between the parameters ensures that their product equals unity. Thus, constraint (6) for parameters can be relaxed since it is fulfilled automatically. Moreover, optimization over three deformation parameters is reduced to optimizing only one parameter $\bar{\mu}_i$ for each object. This choice of parameters is motivated by typical deformation of objects under vertical pressure: changes in height are recompensed by changes in width/length and vice versa. In the second group of instances we set $\mu_i^x, \mu_i^y, \mu_i^z \in R^+, i \in I_n$ and the constraint (6) must be handled explicitly. Comparing with the first group of instances, the runtimes in the second group are typically 1.5–2 times higher (see Tables 1-4 below). Optimized values of $(\mu_i^x)^*, (\mu_i^y)^*, (\mu_i^z)^*, i \in I_n$ for all problem instances are available from the authors upon request.

A computer with a processor 12th Gen Intel(R) Core(TM) i5-12500 3.00 GHz, RAM 32.0 Gb is used for computational experiments. Programming language Python 3.12 is implemented for modeling, while the nonlinear optimization solver IPOPT (Wachter and Biegler (2006)) is used to solve arising optimization problems.

Results reported below were obtained by decomposition Algorithm 2 using starting points generated by Algorithm 1. In all problem instances, we use $\varepsilon = 0.005$ in the stopping criterion at step 7 of Algorithm 2.

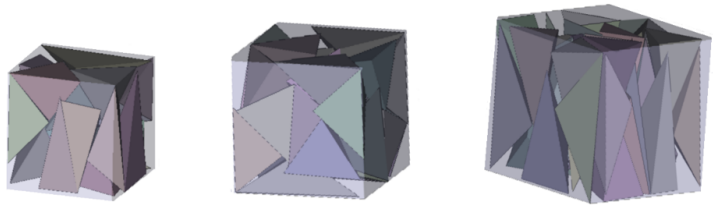
The inputs and outputs to the soft packing problem for tetrahedra with $\mu^- \le \bar{\mu}_i \le \mu^+$ for $i \in I_n$ are provided in Table 1 and with $\mu_i^x, \mu_i^y, \mu_i^z \in R^+$ for $i \in I_n$ are provided in Table 2 for each of containers, respectively.

Table 1
Optimized packing n soft tetrahedra with $\mu^- \le \bar{\mu}_i \le \mu^+$ for $i \in I_n$

n	$\mu^- \le \bar{\mu}_i \le \mu^+$	L	V^*	f^*	runtime (sec)
Tetrahedra in a cuboid					
10	$1 \le \bar{\mu}_i \le 2$	$(a^*, b^*, c^*) = (7.02, 5.65, 7.0)$	277.54	0.5	6.0
20	$0.5 \le \bar{\mu}_i \le 2$	$(a^*, b^*, c^*) = (8.44, 8.44, 7.4)$	527.2	0.53	50.69
30	$0.5 \le \bar{\mu}_i \le 2.5$	$(a^*, b^*, c^*) = (8.96, 8.96, 8.79)$	704.84	0.59	108.71
40	$1.5 \le \bar{\mu}_i \le 2.5$	$(a^*, b^*, c^*) = (10.06, 9.2, 11.16)$	1032.65	0.54	229.43
Tetrahedra in a sphere					
10	$1 \le \bar{\mu}_i \le 2$	$r^* = 4.33$	340.58	0.41	13.18
20	$0.5 \le \bar{\mu}_i \le 2$	$r^* =4.9$	492.38	0.563	16.98
30	$0.5 \le \bar{\mu}_i \le 1.5$	$r^* =5.56$	718.24	0.579	105.83
40	$0.5 \le \bar{\mu}_i \le 2.5$	$r^* =6.11$	957.23	0.579	177.78
Tetrahedra in a cylinder					
10	$1 \le \bar{\mu}_i \le 2$	$(r^*, h^*) = (4.32, 4.32)$	254.16	0.545	4.14
20	$0.5 \le \bar{\mu}_i \le 2$	$(r^*, h^*) = (4.3, 8.6)$	499.28	0.555	36.35
30	$0.5 \le \bar{\mu}_i \le 1.5$	$(r^*, h^*) = (4.77, 9.55)$	683.99	0.61	168.19
40	$0.5 \le \bar{\mu}_i \le 1.5$	$(r^*, h^*) = (5.3, 10.61)$	937.47	0.591	239.12

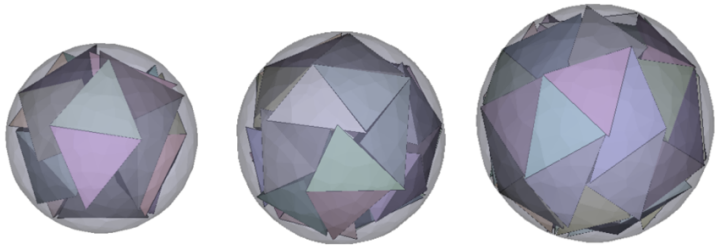
Packing n soft tetrahedra with $\mu^- \le \bar{\mu}_i \le \mu^+$ for $i \in I_n$, obtained by the proposed approach for min-

imal cuboidal, spherical and cylindrical containers are presented in Figures 4, 5 and 6 correspondingly.



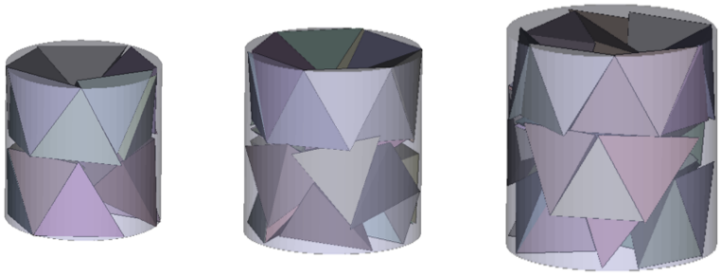
(a) (b) (c)

Fig. 4. Soft tetrahedra in a cuboid for: (a) $n = 20,\ 0.5 \leq \bar{\mu}_i \leq 2$, (b) $n = 30, 0.5 \leq \bar{\mu}_i \leq 2.5$ and (c) $n = 40$, $1.5 \leq \bar{\mu}_i \leq 2.5$.



(a) (b) (c)

Fig. 5. Soft tetrahedra in a sphere for: (a) $n = 20,\ 0.5 \leq \bar{\mu}_i \leq 2$, (b) $n = 30, 0.5 \leq \bar{\mu}_i \leq 1.5$ and (c) $n = 40$, $0.5 \leq \bar{\mu}_i \leq 2.5$.



(a) (b) (c)

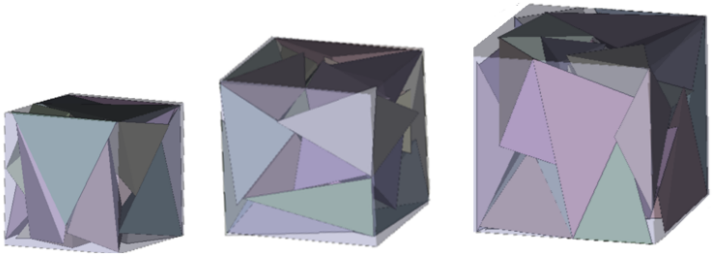
Fig. 6. Soft tetrahedra in a cylinder for: (a) $n = 20,\ 0.5 \leq \bar{\mu}_i \leq 2$, (b) $n = 30, 0.5 \leq \bar{\mu}_i \leq 1.5$, (c) $n = 40, 0.5 \leq \bar{\mu}_i \leq 1.5$.

Packing n soft tetrahedra with $\mu_i^x, \mu_i^y, \mu_i^z \in R^+$ for $i \in I_n$, obtained by the proposed approach for minimal cuboidal, spherical and cylindrical containers are presented in Figures 7, 8 and 9 correspondingly.

The inputs and outputs for soft packing of dodecahedra with $\mu^- \leq \bar{\mu}_i \leq \mu^+$ for $i \in I_n$ are provided in Table 3 and with $\mu_i^x, \mu_i^y, \mu_i^z \in R^+$ are provided in Table 4 for each of containers, respectively.

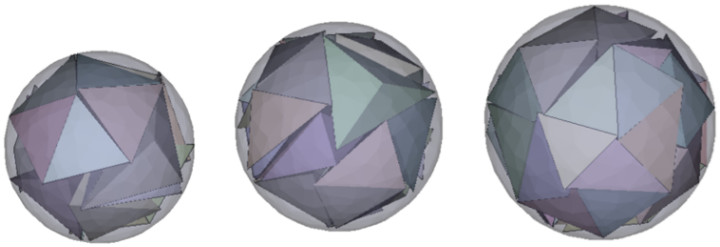
Table 2
Optimized packing n soft tetrahedra with $\mu_i^x, \mu_i^y, \mu_i^z \in R^+$ for $i \in I_n$

n	L	V^*	f^*	runtime (sec)
Tetrahedra in a cuboid				
10	$(a^*, b^*, c^*) = (6.07, 6.07, 6.07)$	224.03	0.61	4.80
20	$(a^*, b^*, c^*) = (7.53, 7.53, 7.53)$	426.70	0.65	25.87
30	$(a^*, b^*, c^*) = (8.61, 8.61, 8.61)$	639.65	0.65	154.85
40	$(a^*, b^*, c^*) = (9.38, 9.38, 9.38)$	826.16	0.67	479.71
Tetrahedra in a sphere				
10	$r^* = 4.33$	349.00	0.40	3.52
20	$r^* = 4.94$	501.78	0.55	19.16
30	$r^* = 5.48$	689.13	0.60	106.10
40	$r^* = 5.91$	865.60	0.64	373.90
Tetrahedra in a cylinder				
10	$(r^*, h^*) = (4.0, 5.032)$	252.93	0.548	8.80
20	$(r^*, h^*) = (4.0, 9.65)$	485.34	0.57	45.45
30	$(r^*, h^*) = (5.45, 7.09)$	662.00	0.63	205.14
40	$(r^*, h^*) = (5.9, 7.66)$	838.16	0.66	481.16



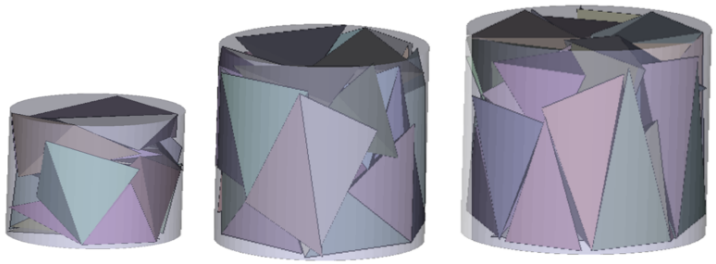
(a) (b) (c)

Fig. 7. Soft tetrahedra in a cuboid for: (a) $n = 20$, (b) $n = 30$ and (c) $n = 40$.



(a) (b) (c)

Fig. 8. Soft tetrahedra in a sphere for: (a) $n = 20$, (b) $n = 30$ and (c) $n = 40$.



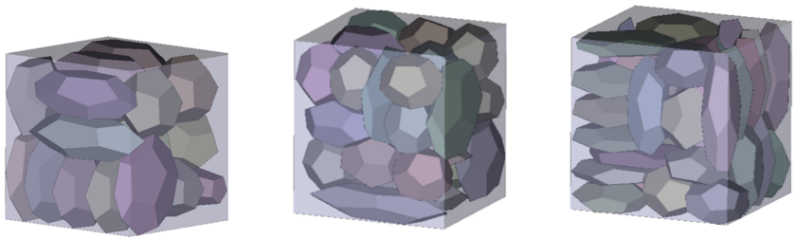
(a) (b) (c)

Fig. 9. Soft tetrahedra in a cylinder for: (a) $n = 20$, (b) $n = 30$, (c) $n = 40$.

Table 3
Optimized packing n soft dodecahedra with $\mu^- \leq \bar{\mu}_i \leq \mu^+$ for $i \in I_n$

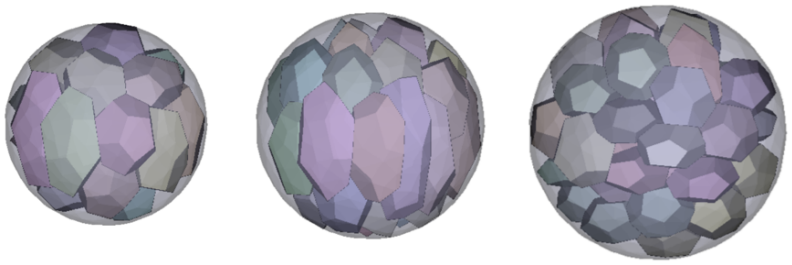
n	$\mu^- \leq \bar{\mu}_i \leq \mu^+$	L	V^*	f^*	runtime (sec)
Dodecahedra in a cuboid					
10	$0.5 \leq \bar{\mu}_i \leq 1.5$	$(a^*, b^*, c^*) = (7.69, 8.31, 7.08)$	452.62	0.49	84.18
20	$0.5 \leq \bar{\mu}_i \leq 2$	$(a^*, b^*, c^*) = (9.52, 9.22, 9.81)$	862.65	0.52	250.45
30	$0.5 \leq \bar{\mu}_i \leq 2.5$	$(a^*, b^*, c^*) = (11.9, 11.92, 11.88)$	1229.9	0.54	860.74
40	$0.5 \leq \bar{\mu}_i \leq 2$	$(a^*, b^*, c^*) = (11.9, 11.92, 11.88)$	1685.6	0.53	1173.4
Dodecahedra in a sphere					
10	$1 \leq \bar{\mu}_i \leq 2$	$r^* = 4.68$	430.94	0.52	28.8
20	$0.5 \leq \bar{\mu}_i \leq 2$	$r^* = 5.73$	789.63	0.56	132.9
30	$1.5 \leq \bar{\mu}_i \leq 1.5$	$r^* = 6.68$	1248.4	0.54	529.93
40	$0.5 \leq \bar{\mu}_i \leq 2.5$	$r^* = 7.26$	1602.6	0.56	1530.02
Dodecahedra in a cylinder					
10	$1 \leq \bar{\mu}_i \leq 2$	$(r^*, h^*) = (4.25, 8.51)$	483.71	0.46	68.84
20	$0.5 \leq \bar{\mu}_i \leq 2$	$(r^*, h^*) = (6.63, 6.34)$	876.9	0.51	748.05
30	$0.5 \leq \bar{\mu}_i \leq 1.5$	$(r^*, h^*) = (6.62, 8.6)$	1185.48	0.56	908.66
40	$0.5 \leq \bar{\mu}_i \leq 1.5$	$(r^*, h^*) = (6.36, 12.72)$	1618	0.55	1069.61

Packing n soft dodecahedra with $\mu^- \leq \bar{\mu}_i \leq \mu^+$ for $i \in I_n$, obtained by the proposed approach for minimal cuboidal, spherical and cylindrical containers are presented in Figures 10, 11 and 12 correspondingly.



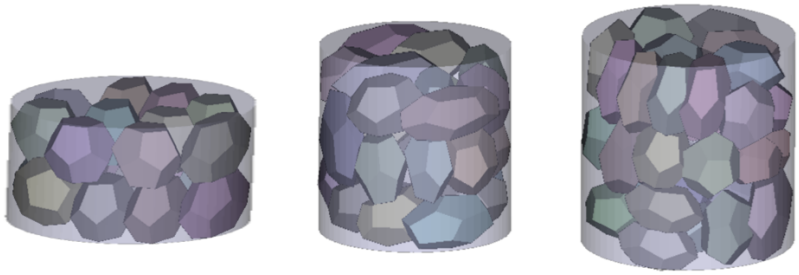
(a) (b) (c)

Fig. 10. Soft dodecahedra in a cuboid for: (a) $n = 20,\ 0.5 \leq \mu_i \leq 2$; (b) $n = 30,\ 0.5 \leq \mu_i \leq 2.5$; (c) $n = 40$, $0.5 \leq \mu_i \leq 2$.



(a) (b) (c)

Fig. 11. Soft dodecahedra in a sphere for: (a) $n = 20,\ 0.5 \leq \mu_i \leq 2$; (b) $n = 30,\ 1.5 \leq \mu_i \leq 2.5$; (c) $n = 40$, $0.5 \leq \mu_i \leq 2.5$.



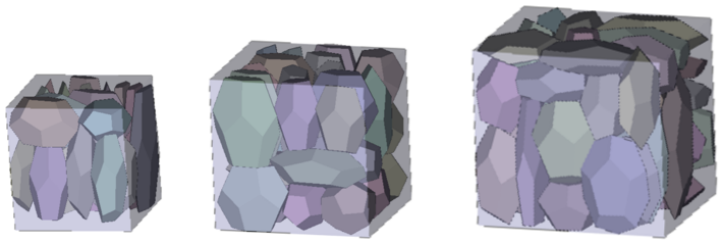
(a) (b) (c)

Fig. 12. Soft dodecahedra in a cylinder for: (a) $n = 20,\ 0.5 \leq \mu_i \leq 2$; (b) $n = 30,\ 0.5 \leq \mu_i \leq 1.5$; (c) $n = 40$, $0.5 \leq \mu_i \leq 2.5$.

Table 4
Optimized packing n soft dodecahedra with $\mu_i^x, \mu_i^y, \mu_i^z \in R^+$ for $i \in I_n$

n	L	V^*	f^*	runtime (sec)
Dodecahedra in a cuboid				
10	$(a^*, b^*, c^*) = (7, 41, 7.41, 7.41)$	406.46	0.55	80.59
20	$(a^*, b^*, c^*) = (9.29, 9.29, 9.29)$	802.32	0.56	199.67
30	$(a^*, b^*, c^*) = (10.54, 10.54, 10.54)$	1170.00	0.57	386.63
40	$(a^*, b^*, c^*) = (11.51, 11.51, 11.51)$	1526.67	0.58	1036.90
Dodecahedra in a sphere				
10	$r^* = 4.58$	401.32	0.56	17.21
20	$r^* = 5.66$	762.67	0.58	260.98
30	$r^* = 6.48$	1136.68	0.59	795.91
40	$r^* = 7.07$	1479.38	0.60	1831.35
Dodecahedra in a cylinder				
10	$(r^*, h^*) = (4.55, 5.92)$	385.92	0.577	21.11
20	$(r^*, h^*) = (5.68, 7.38)$	748.22	0.596	204.90
30	$(r^*, h^*) = (6.22, 9.32)$	1131.98	0.59	991.02
40	$(r^*, h^*) = (6.76, 10.14)$	1455.30	0.61	1872.45

Packing n soft dodecahedra with $\mu_i^x, \mu_i^y, \mu_i^z \in R^+$ for $i \in I_n$ obtained by the proposed approach for minimal cuboidal, spherical and cylindrical containers are presented in Figures 13, 14 and 15 correspondingly.

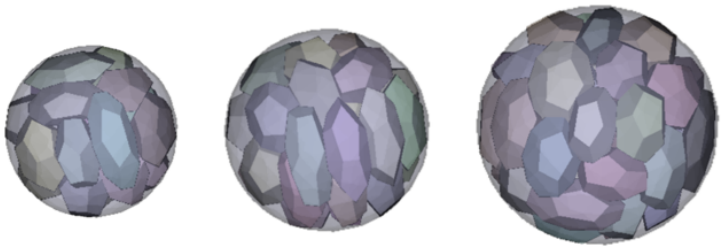


(a) (b) (c)

Fig. 13. Soft dodecahedra in a cuboid for: (a) $n = 20$, (b) $n = 30$ and (c) $n = 40$.

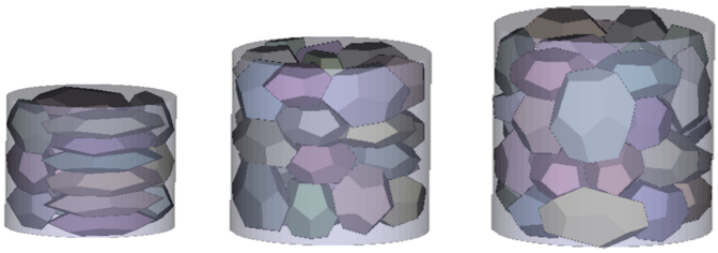
From Tables 1–4 we may conclude that achieved filling factors are moderate, $0.4 - 0.67$ for tetrahedra and $0.5 - 0.6$ for dodecahedra. The best-known theoretical estimations of filling factors for regular polyhedra are up to 0.8563 for tetrahedra (Chen et al. (2010)) and up to 0.716 for dodecahedra (Jiao and Torquato (2011)). However, these results were obtained for packing thousands of regular polyhedra in an "open space", without considering containment constraints.

Consider an illustrative example of packing 12 equal regular dodecahedra in a minimal height cuboidal container. The fixed rectangular base of the container has dimensions $a = 8$, $b = 8$. The problem (3)-(7) is solved by the global solver BARON (Tawarmalani and Sahinidis (2005)) for rigid objects



(a) (b) (c)

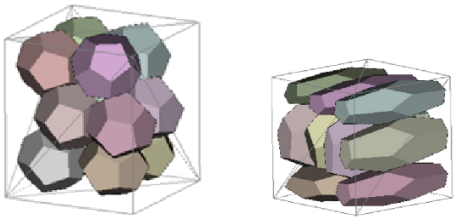
Fig. 14. Soft dodecahedra in a sphere for: (a) $n = 20$, (b) $n = 30$ and (c) $n = 40$.



(a) (b) (c)

Fig. 15. Soft dodecahedra in a cylinder for: (a) $n = 20$, (b) $n = 30$, (c) $n = 40$.

($\mu_i = (1, 1, 1)$ for $i \in I_n$) under free translations and rotations. The best feasible solution (*Upper bound*) found by the global solver BARON is $c^* = 9.3276605236185528$ with the corresponding *Lower bound* $= 9.3275669482421875$. This configuration is presented in Figure 16a. The corresponding filling factor is $f^* = 0.4479$. The best feasible solution obtained by our approach for soft dodecahedra is provided in Figure 16b with $c^* = 7.5885$ and $f^* = 0.55$. Here deformation parameters are nonnegative, and constraint (6) is handled explicitly.



(a) (b)

Fig. 16. (a) $V^* = 596.97,\ c^* = 9.3276605236185528,\ f^* = 0.4479$, (b) $V^* = 485.67,\ c^* = 7.5885,\ f^* = 0.55$.

As an example of efficiency of the decomposition approach, a comparative solution to three problem instances is reported in Table 5. Here solutions are presented for packing $n = 60$ soft tetrahedra in a minimum-volume cuboidal, spherical and cylindrical container obtained with and without decomposition for the same starting points.

In both cases, Algorithm 1 is first used to generate a feasible initial solution. In the case with decomposition, Algorithm 2 is subsequently applied, taking this feasible solution as its starting point. In

Table 5
Packing $n = 60$ soft tetrahedra in a minimum-volume container

$\mu^- \leq \bar{\mu}_i \leq \mu^+$	Approach	L	V^*	f^*	runtime (sec)
Cuboidal container					
$1.5 \leq \bar{\mu}_i \leq 2.5$	without decomposition	$(a^*, b^*, c^*) = (12.6, 10.53, 11.57)$	1579.83	0.53	1616.38
	with decomposition	$(a^*, b^*, c^*) = (12.017, 10.456, 11.673)$	1466.57	0.57	940.37
Spherical container					
$0.5 \leq \bar{\mu}_i \leq 2$	without decomposition	$r^* = 7.0$	1436.76	0.57	672.14
	with decomposition	$r^* = 6.982$	1425.53	0.58	475.68
Cylindrical container					
$1 \leq \bar{\mu}_i \leq 2$	without decomposition	$(r^*, h^*) = (6.19, 12.38)$	1488.58	0.559	2054.89
	with decomposition	$(r^*, h^*) = (6.14, 12.27)$	1451.08	0.57	1245.97

contrast, in the case without decomposition, Algorithm 2 is not used; instead, IPOPT is applied directly to the feasible solution obtained by Algorithm 1 to compute a local optimum of problem (3)–(7). Thus, the difference in computational times arises from the use (or absence) of the decomposition procedure in Algorithm 2.

As can be seen from Table 5 and Table 6, the decomposition approach permits obtaining better and faster solutions. Time savings depend on starting points used and the container type.

Considering the multistart nature of the proposed solution approach, it is interesting to see how the choice of starting points affects the final solution. For packing $n = 40$ soft dodecahedra in an optimized cuboid with $0.5 \leq \bar{\mu}_i \leq 2$, 50 starting points are randomly generated. For each starting point the optimal volume of the container and corresponding total runtime are analyzed. The obtained mean value of the optimal volume is 1731.577 with the standard deviation 36.16003. For the runtime, the obtained mean value is 2308.865, the standard deviation 716.0289. Corresponding relative coefficient of variation for the optimal volume is 2.088272%, while the coefficient of variation of the runtime is 31.01216%. Thus, we may conclude that the choice of starting point affects significantly the runtime, while the optimal objective is almost independent. Detailed results of this experiment are available from the authors on request.

Table 6
Packing $n = 40$ soft dodecahedra in a minimum-volume container

$\mu^- \le \bar{\mu}_i \le \mu^+$	Approach	L	V^*	f^*	runtime (sec)
Cuboidal container					
$0.5 \le \bar{\mu}_i \le 2$	without decomposition	$(a^*, b^*, c^*) = (12.71, 7.01, 19.27)$	1717.83	0.52	2696.94
	with decomposition	$(a^*, b^*, c^*) = (11.9, 11.92, 11.88)$	1685.6	0.53	1173.4
Spherical container					
$0.5 \le \bar{\mu}_i \le 2.5$	without decomposition	$r^* = 7.35$	1662.5	0.54	1906.23
	with decomposition	$r^* = 7.26$	1602.5	0.54	1530.02
Cylindrical container					
$0.5 \le \bar{\mu}_i \le 2.5$	without decomposition	$(r^*, h^*) = (6.38, 12.75)$	1628.44	0.55	1715.93
	with decomposition	$(r^*, h^*) = (6.36, 12.72)$	1618.0	0.55	1069.61

5. A case study – digital model of a natural core

During the operation of oil wells, their flow rates usually decrease. The reason is not only in a reservoir pressure drop but also in a decrease of the ability of a porous medium to transmit fluids (permeability), especially in the zone immediately surrounding a wellbore (bottomhole formation zone) (Blunt (2017); Kravchenko et al. (2019)). The productivity of such wells can be restored by applying various oil production enhancement methods (Gerke et al. (2021); Kravchenko et al. (2023b)). To determine experimentally the permeability change, cylindrical rock samples extracted from subterranean formations (natural cores) can be used. They are a source of specific information about the reservoir rock and the character of fluid filtration therein. However, extraction of core rock from a productive formation without damaging it is a complex and expensive process. Therefore, cores are either available in limited quantities or are completely absent.

To cope with this problem, experimental studies are carried out on artificial cores made by special technologies. It is very important that artificial cores have morphological, mineralogical, and filtration-capacity properties as close as possible to those of natural cores. To produce artificial cores that simulate the compression effect and permeability anisotropy, the prepared powder mass (sandstones and plasticizing binder) is pressed at a temperature of 120-140°C. This temperature level reduces the viscosity of the binder and allows for the deformation of the composite particles without fracture, while using the pressing pressure 1.3-1.4 tons per cm^2 changes the original shapes of the particles. To create a model of the artificial core the optimized packing approach proposed in the previous section is used. It is assumed that the reservoir is granular, i.e. a porous one. The rock grains (particles) have a polyhedral shape and are packed in a circular cylinder (container).

The actual data for our case study is obtained by petrophysical studies of real natural cores (Kravchenko et al. (2023a)) and are presented in Table 7. The third column provides information on fractions sizes, while the last column gives a volumetric ratio for each fraction. The following notations

are used: k is the type of rock grains, $d^{(k)} \in [d^{-(k)},\ d^{+(k)}]$ is the k-th type grain diameter, $\tau^{(k)}$= (total volume of the k-th type particles)/(total volume of particles) is the ratio of appearance of the grains (particles) in the natural core (container).

The modeling is aimed at refining the fractional composition to create a model core with specified porosity parameters. Here the porosity is defined as a relative value of unfilled space of the container, $(1 - f^*)$, where f^* is a filling factor defined in Section 4.

Table 7
Actual data obtained by petrophysical studies of real natural cores

#	Composition	$d^{(k)} \in [d^{-(k)}, d^{+(k)}]$ (mm), $k = 1, .., 7$	Content (ratio), $\tau^{(k)}$, $k = 1, .., 7$
1	Coarse-grained sandstone	0.5-1.0	0.04
2	Medium-grained sandstone	0.25-0.5	0.02
3	Fine-grained sandstone	0.1-0.25	0.44
4	Aleurolitic coarse-grained	0.05-0.1	0.06
5	Fine-grained aleurolitic	0.01-0.05	0.18
6	Pelitic	0.001-0.01	0.09
7	Ultrafine-grained sandstone	0.001-0.005	0.17

In the experimental study an optimized packing of $n = 200$ soft dodecahedral particles in a circular cylinder with $r = 5.56\ mm$ and the deformation parameter limits $\bar{\mu}_i^- = 1$, $\bar{\mu}_i^+ = 2$ is considered to minimize the height of the container. The deformation parameters are limited, but no specific relation between parameters is assumed, i.e. constraint (6) is handled explicitly. In this sense the experimental design is similar to the second group of problem instances in Section 4. Note that dodecahedral shapes are frequently used in complex systems modeling (see, e.g., Li et al. (2020); Jenczyk (2024)).

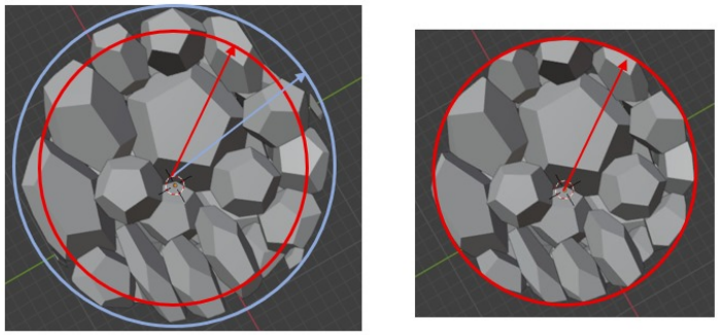
Initially all particles have the shape of regular dodecahedra with regular pentagonal facets. Particles inside each of the 7 types have the same diameters selected randomly from the corresponding intervals $[d^{(k)-},\ d^{(k)+}]$ defined in Table 7.

The number of particles n_k for each of the seven types is calculated directly from the corresponding volume fractions $\tau^{(k)}$ given in Table 7: $n_k = n \cdot \tau^{(k)}$, where $n = 200$. In the example, $n_1 = 8, n_2 = 4, n_3 = 88, n_4 = 12, n_5 = 36, n_6 = 18, n_7 = 34$. The particles within each type are assigned diameters selected randomly from the corresponding interval $[d^{(k)-},\ d^{(k)+}]$. The particles are numbered as follows: type 1 (coarse-grained sandstone) $i = 1, ..., 8$; type 2 (medium-grained sandstone) $i = 9, ..., 12$; type 3 (fine-grained sandstone) $i = 13, ..., 100$; type 4 (aleurolitic coarse-grained) $i = 101, ..., 112$; type 5 (fine-grained aleurolitic) $i = 113, ..., 148$; type 6 (pelitic) $i = 149, ..., 166$, type 7 (ultrafine-grained sandstone) $i = 167, ..., 200$. Note that the volume of each particle remains constant under deformation.

Two variants of the main problem are considered. In the first case the principal objective is modeling the porous structure like that obtained by scanning electron microscopy. The corresponding problem (3)–(7) is solved by the decomposition approach using the data presented in Table 7.

In the second case the focus is on modeling natural cores obtained by cutting a core from a rock structure using a special sharp diamond tool. The principal difference is that here a so-called border-wall effect arises since particles close to the core boundary can be truncated by the sharp tool. Correspondingly, only parts of these particles' volumes must be considered in the porosity estimations.

This border-wall effect is handled as follows. First, optimal packing of soft particles is obtained without considering the border-wall effect, but for a cylindrical container with a larger radius $r(1+\Delta),\ \Delta > 0$. Then, particles laying partially outside the original container are detected. This is done by simply verifying if the containment conditions (5) stated for the original radius r are violated. For a particle with violated containment condition the volume of its part laying inside the original container is calculated. This volume is then used in porosity calculation. The main concepts of quasi-packing are illustrated in Figure 17.



(a) (b)

Fig. 17. Illustration of the quasi-packing approach.

The view from above on particles in a cylindrical container is presented in Figure 17. The red circle corresponds to the original container of radius r, while the the larger blue circle represents the expanded container of radius $r(1+\Delta)$. Optimal packing in the expanded container is provided in Figure 17a. Corresponding quasi-packing in the original container with truncated particles near the boundary is given in Figure 17b.

The phi-function used in the containment condition (5) is changed for a larger radius $r(1+\Delta),\ \Delta > 0$ as follows:

$$\psi_i^{\Delta}(u_i, \mu_i, r, h) = \min\{\min_{k\in J_i}(r^2(1+\Delta)^2 - (x_i^k)^2 - (y_i^k)^2),\ \min_{k\in J_i} z_i^k,\ \min_{k\in J_i}(-z_i^k + h)\}.$$

Corresponding changes must be made to those stages of the main algorithm where the containment conditions are used.

Volume of the particle part left inside the original container after truncation is calculated using the open-access library https://trimesh.org/ (Dawson-Haggerty, M. et al. (2019)). First, a mesh with certain accuracy is generated for the cylindrical container obtained by optimization, as well as for all dodecahedra with violated containment conditions. Then the volume of the intersection of the mesh cylindrical container and mesh dodecahedra is calculated using Boolean operations on mesh to represent intersection of two mesh objects (see Dawson-Haggerty, M. et al. (2019) for more details).

The results obtained by the proposed solution approach are presented in Figure 18. Here Figure 18a and Figure 18c provide starting feasible points for cases 1 and 2, correspondingly. Solutions obtained by the proposed approach for cases 1 and 2 are demonstrated in Figure 18b and Figure 18d. For quasi-packing approach $\Delta = 0.25$ is used.

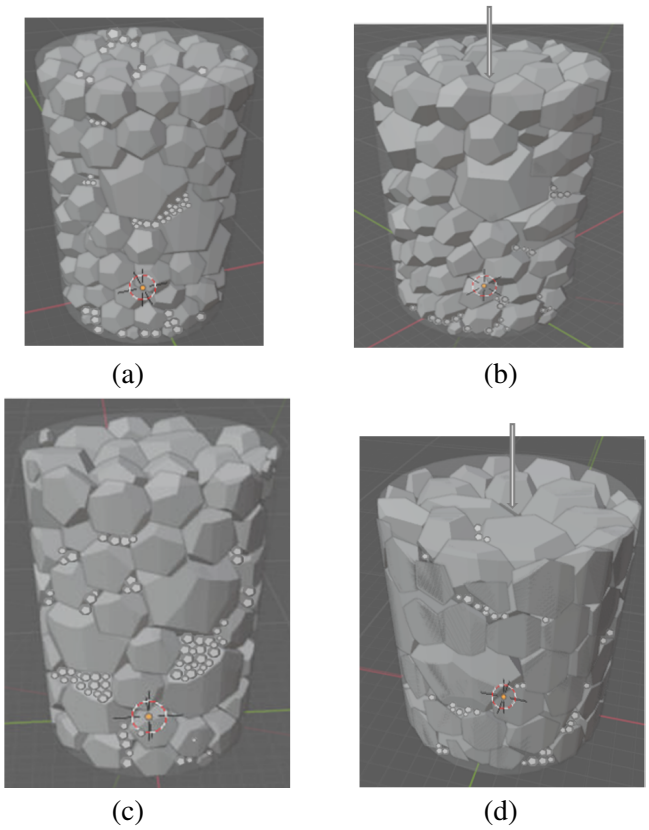


Fig. 18. Optimized packings for modeling digital core: (a) $r = 0.556$, $h^* = 1.668$, $\bar{\mu}_i = 1$, $f^* = 0.5679$, runtime $= 18839.32$ sec; (b) $r = 0.556$, $h^* = 1.584$, $1 \leq \bar{\mu}_i \leq 2$, $f^* = 0.6$, runtime $= 51927.92$ sec; (c) $r = 0.519$, $h^* = 1.558$, $\bar{\mu}_i = 1$, $f^* = 0.63$, runtime $= 39462.8$ sec; (d) $r = 0.519$, $h^* = 1.085$, $1 \leq \bar{\mu}_i \leq 2$, $f^* = 0.72$, runtime $= 42999.92$ sec.

For the natural core with characteristics summarized in Table 7, the experimental value of porosity $1 - f^*$ is 29.4%. The value of porosity obtained without considering the border-wall effect (Figure 18(b) is 40%. If the border-wall effect is considered (Figure 18(d) the values of the porosity is reduced to 28%, which is very close to experimental results. Note, that in (Kravchenko et al. (2023a)) the particles are approximated by different-sized spheres and even considering the border-wall effect (quasi packing) the porosity obtained by modeling differs from experimental value in more than 10%. A principal difference of our approach from that model is not only in considering the polyhedral shapes of the particles, but in the possibility to describe the anisotropy of permeability in the vertical and horizontal directions. Typically, horizontal permeability is greater than vertical permeability. This is due to the process of layer-by-layer formation of sedimentary rocks with subsequent deformation of individual fractions due to compression in the vertical direction. The deforming transformation of the soft particles considered in this paper permits modeling of these anisotropy effects and thus increases the compatibility with experimental results. We may conclude that using computer modeling tools based on optimized packing soft polyhedra, a granular structure has been designed tightly approximating results of experimental petrophysical studies.

6. Conclusions

The problem of arranging soft polyhedra in a minimal volume convex container is considered. Soft polyhedra can change their shapes within certain limits subject to their volume and convexity preservation. Polyhedral objects can be freely translated/rotated and must be placed into a container without overlapping. The objective is to define the values of the deformation parameters and positions of the polyhedra to feet in the minimal volume container. Mathematical modeling tools to formulate analytically placement conditions for soft polyhedra are proposed: phi-functions are used to state containment conditions, while quasi phi-functions are implemented to ensure non-overlapping of soft polyhedra. A mathematical model for optimized packing soft convex polyhedra is proposed and a corresponding nonlinear nonconvex programming problem is formulated. A multistart heuristic solution strategy is developed based on generating feasible starting points and decomposing the original large-scale problem into a sequence of subproblems of smaller dimension. Computational results for arranging soft tetrahedra and dodecahedra in rectangular, spherical and cylindrical containers are presented to demonstrate efficiency of the proposed solution approach.

The proposed approach is used to design an artificial core based on petrophysical studies of real natural cores. Particles of the real core are approximated by soft dodecahedra of different sizes, while cylindrical core (container) is considered. It is demonstrated that the granular structure and porosity of the artificial core are very close to those of the natural one.

In what follows we would like to highlight some directions for future research. These directions can be considered as natural generalizations of the proposed approach and do not require significant changes in the proposed modeling and solution scheme.

A special shape transformation represented by a diagonal deformation matrix is used in this paper to guarantee volume preservation of polyhedral objects. However, as follows from the demonstration of Proposition 1, more general deformation matrices can be considered without breaking the volume preservation. Using general shape transformations can increase geometric diversity of soft objects. In the paper deformation is applied before rotation thus maintaining the shape of the transformed object similar to that of the original one. This is motivated by the specific core application where objects are basically deformed under vertical pressure. Considering deformations not aligned with principal axes would increase the modelling flexibility (see Litvinchev et al. (2024b) for 2D case).

In many physical systems, the volumes of the objects are not conserved and can be either reduced due to freezing/evaporation or increased because of heating/extension. This situation can also be modelled by the proposed approach allowing the determinant of the shape transformation matrix to be different from unity.

Packing problems in higher dimensions have various interpretations, e.g., in project management and scheduling (see, e.g., Zhang (2004); Fasano (2014)) where dimensions of the object are defined by the number of resources used by the project. Modeling and solving multidimensional soft packing problems is an interesting area for future research.

The proposed approach can be further extended to the packing of irregular 3D soft objects composed of convex 3D shapes (Pankratov et al. (2020); Litvinchev et al. (2024a)). Some results in these directions are on the way. It is also interesting to revise online packing formulations and algorithms (Ali et al. (2022, 2024, 2025)) for soft 3D objects.

In most problem instances of digital core modeling the runtimes are high. This is caused by the

large-scale nature of the main optimization problem (3)–(7). Although the core problem typically is not solved in real time, high runtimes may limit practical applicability. One of limitations of the proposed heuristic solution approach is the lack of suboptimality bounds that can be useful to improve the convergence. Using the special structure of the optimization problem (3)–(7) to construct efficient decomposition/aggregation techniques and/or derive bounds for the optimal value (see, e.g., Litvinchev and Tsurkov (2003)) can reduce runtimes and strengthen the proposed heuristic solution technique.

Acknowledgments

This study is supported by the British Academy (Grant #100072) for the first author and the European Union for the last author.

References

Ali, S., Ramos, A.G., Carravilla, M.A., Oliveira, J.F., 2022. On-line three-dimensional packing problems: A review of off-line and on-line solution approaches. *Computers & Industrial Engineering* 168, 108122.

Ali, S., Ramos, A.G., Carravilla, M.A., Oliveira, J.F., 2024. Heuristics for online three-dimensional packing problems and algorithm selection framework for semi-online with full look-ahead. *Applied Soft Computing* 151, 111168.

Ali, S., Ramos, A.G., Oliveira, J.F., 2025. Static stability versus packing efficiency in online three-dimensional packing problems: A new approach and a computational study. *Computers & Operations Research* 178, 107005.

Alliez, P., Cohen-Steiner, D., Yvinec, M., Desbrun, M., 2005. Variational tetrahedral meshing. In *ACM SIGGRAPH 2005 Papers (SIGGRAPH '05)*, Association for Computing Machinery, New York, NY, USA, pp. 617–625.

Alvarez-Valdés, R., Carravilla, M.A., Oliveira, J.F., 2025. Cutting and packing. In Martí, R., Pardalos, P.M. and Resende, M.G. (eds), *Handbook of Heuristics*. Springer, Cham.

Araújo, L.J.P., Özcan, E., Atkin, J.A.D., Baumers, M., 2018. Analysis of irregular three-dimensional packing problems in additive manufacturing: a new taxonomy and dataset. *International Journal of Production Research* 57, 18, 5920–5934.

Bennell, J., Litvinchev, I., Pankratov, A., Romanova, T., 2024. Packing stretched convex polygons in an optimized rectangle. *Wireless Networks*. doi: 10.1007/s11276-023-03642-9.

Blunt, M.J., 2017. *Multiphase Flow in Permeable Media: A Pore-Scale Perspective*. Cambridge University Press.

Bronshtein, I., Semendyayev, K., Musiol, G., Mühlig, H., 2015. *Handbook of Mathematics* (6th edn.). Springer, Berlin, Heidelberg, New York.

Chehrazad, S., Roose, D., Wauters, T., 2025. A fast and scalable deepest-left-bottom-fill algorithm to solve irregular 3D cutting and packing problems using a semi-discrete representation. *International Journal of Production Research*. pp. 1–24.

Chen, E.R., Engel, M., Glotzer, S.C., 2010. Dense crystalline dimer packings of regular tetrahedra. *Discrete & Computational Geometry* 44, 253–280.

Chen, M., Peng, X., Tang, X., 2025. Filtered beam search algorithm for the two-dimensional rectangular packing problem. *International Transactions in Operational Research* 32, 6, 3729–3755.

Chen, Y., Yuan, M., Wang, Z., Zhao, Y., Li, J., Hu, B., Xia, C., 2021. Structural characterization and statistical properties of jammed soft ellipsoid packing. *Soft Matter* 17, 2963.

Chernov, N., Stoyan, Y., Romanova, T., 2010. Mathematical model and efficient algorithms for object packing problem. *Computational Geometry* 43, 535–553.

Conway, J., Torquato, S., 2006. Packing, tiling, and covering with tetrahedra. *Proc. Natl. Acad. Sci. U.S.A.* 103, 28, 10612–10617.

Coutinho, J., Reis, M., Gonçalves Neves, D., Bernardo, F., 2023. Robust optimization and data-driven modeling of tissue paper packing considering cargo deformation. *Computers & Industrial Engineering* 175, 108898.

Dahle, L., Vaswani, P., Bhatia, D., 2023. Tetrahedral dna nanocages as delivery agent for biological and biomedical applications.

Nano and Medical Materials 3, 1, 151.

Dawson-Haggerty, M. et al., 2019. Trimesh. Software. Version 3.2.0, https://trimesh.org/.

Du, S., Liu, M., Nie, T., Zhu, Y., 2024. Package-type strategies and packaging's carbon reduction decisions in the take-out industry. *International Journal of Production Research* 62, 18, 6542–6572.

Fasano, G., 2014. *Solving Non-Standard Packing Problems by Global Optimization and Heuristics*. Springer, Cham, Switzerland.

Fasano, G., Pintér, J.D., 2016. *Modeling and Optimization with Case Studies*, *Springer Optimization and Its Applications: Space Engineering*. Vol. 114. Springer.

Fischer, A., Scheithauer, G., 2015. Cutting and packing problems with placement constraints. In Fasano, G. and Pintér, J. (eds), *Optimized Packings with Applications*. Springer, Cham, Switzerland, pp. 119–156.

Gerke, K., Korost, D., Karsanina, M., Korost, S., Vasiliev, R., Lavrukhin, Y., Gafurova, D., 2021. The studying and analysis of modern approaches to building core digital models and the methods of modeling multiphase filtration on a pore space scale. *Georesursy* 23, 2, 197–213.

Gou, D., An, X., Zhao, B., Yang, R., 2020. Cfd-dem simulations of densification of tetrahedron particles under air impact. *Powder Technology* 361, 220–225.

Guo, R., Li, J., Ai, B., 2023. Melting of two-dimensional deformable particle systems. *Physica A: Statistical Mechanics and its Applications* 623, 128833.

Hadj Salem, K., Silva, E., Oliveira, J.F., 2023. Cutting and packing problems under uncertainty: literature review and classification framework. *International Transactions in Operational Research* 30, 6, 3329–3360.

Hartmann, S., 2000. Packing problems and project scheduling models: an integrating perspective. *J Oper Res Soc* 51, 1083–1092.

Januszewski, J., Zielonka, L., 2024. Packing a tetrahedron by similar tetrahedra. *Results in Mathematics / Resultate der Mathematik* 79, 2.

Jenczyk, J., 2024. Regular dodecahedron-based network structures. *Symmetry* 16, 11, 1509.

Ji, P., He, K., Jin, Y., Lan, H., Li, C., 2017. An iterative merging algorithm for soft rectangle packing and its extension for application of fixed outline floorplanning of soft modules. *Comput Oper Res* 86, 110–123.

Jiang, J., Garikipati, K., Rudraraju, S., 2019. A diffuse interface framework for modeling the evolution of multi-cell aggregates as a soft packing problem driven by the growth and division of cells. *Bull Math Biol* 81, 3282–3300.

Jiao, Y., Torquato, S., 2011. Maximally random jammed packings of platonic solids: Hyperuniform long-range correlations and isostaticity. *Physical Review E* 84, 4, 041309.

Kallrath, J., Ryu, J., Song, C., Lee, M., Kim, D., 2021. Near optimal minimal convex hulls of disks. *J Glob Optim* 80, 551–594.

Kim, S., Gee, K., Hart, A., 2024. A bayesian sampling framework for constrained optimisation of build layouts in additive manufacturing. *International Journal of Production Research* 62, 16, 5772–5790.

Kravchenko, O., Romanova, T., Veligotskyi, D., Homan, V., Agayev, U., Yaskov, G., Chuhai, A., 2023a. Methodology of creation of artificial core reservoir formations using geometric design methods. In *SPE Caspian Technical Conference and Exhibition*, Baku, Azerbaijan.

Kravchenko, O., Veligotskyi, D., Bashtovyi, A., Veligotska, Y., 2019. Improving the controllability and effectiveness of the chemical-technological process of the technology for hydrogen thermobaric chemical stimulation of hydrocarbon recovery. *Eastern-European Journal of Enterprise Technologies* 6, 6, 57–66. Issue 102.

Kravchenko, O., Veligotskyi, D., Homan, V., Baranov, I., 2023b. Increasing the effectiveness of the complex hydrogen thermobaric chemical effect technology for stimulation of the production of hydrocarbons by using polymer paracyanogen. *International Journal of Energy for a Clean Environment* 24, 7, 135–147.

Leao, A.A.S., Toledo, F.M.B., Oliveira, J.F., Carravilla, M.A., Alvarez-Valdés, R., 2020. Irregular packing problems: A review of mathematical models. *European Journal of Operational Research* 282, 3, 803–822.

Lewis, B., Robinson, J., 1978. Triangulation of planar regions with applications. *Comput J* 21, 4, 324–332.

Li, J., An, X., Wang, J., Zhao, H., Zou, R., Dong, K., Gou, D., 2020. Experimental study on 3D vibrated packing densification of mono-sized dodecahedral particles. *Powder Technology* 367, 703–712.

Litvinchev, I., Fischer, A., Romanova, T., Stetsyuk, P., 2024a. A new class of irregular packing problems reducible to sphere packing in arbitrary norms. *Mathematics* 12, 935.

Litvinchev, I., Infante, L., Romanova, T., Martinez-Noa, A., Gutierrez, L., 2024b. Packing soft convex polygons in an optimized convex container. *Mobile Networks and Applications* 29, 211–220.

Litvinchev, I., Tsurkov, V., 2003. *Aggregation in Large-Scale Optimization*. (1st edn.). Springer New York, NY.

Lu, F., Zhang, Y., Dwyer, T., Michelson, A., Moore, T., Yan, H., Kisslinger, K., Zhang, H., Chen, X., Glotzer, S., Gang, O., 2025. Octo-diamond crystal of nanoscale tetrahedra with interchanging chiral motifs. *Nature Materials* 24, 5, 785–793.

Ma, W., Zhang, B., Han, L., Huo, S., Wang, H., Navarro-Alarcon, D., 2023. Action planning for packing long linear elastic objects into compact boxes with bimanual robotic manipulation. *IEEE/ASME Trans Mechatron* 28, 3, 1718–1729.

Melashenko, O., Romanova, T., Litvinchev, I., Martínez Gomez, C., Yang, R., Sun, B., 2025. A model-based heuristic for packing soft rotated rectangles in an optimized convex container with prohibited zones. *Mathematics* 13, 493.

Moghaddam, T., Baaj, H., 2018. Application of compressible packing model for optimization of asphalt concrete mix design. *Construction and Building Materials* 159, 530–539.

Murata, H., Kuh, E., 1998. Sequence-pair based placement method for hard/soft/preplaced modules. In *International Symposium on Physical Design (ISPD1998)*, Monterey, CA, USA, pp. 167–172.

Oliveira, O., Gamboa, D., Silva, E., 2023. An introduction to the two-dimensional rectangular cutting and packing problem. *International Transactions in Operational Research* 30, 6, 3238–3266.

Pankratov, A., Romanova, T., Litvinchev, I., 2020. Packing oblique 3D objects. *Mathematics* 8, 7, 1130.

Ponomarev, A., Kadyrov, I., Tugushev, O., Drugov, D., Vaganov, Y., Leontiev, D., Zavatsky, M., 2022. Digital core reconstruction research: challenges and prospects. *Geology, Ecology, and Landscapes* 8, 1, 49–56.

Qian, Y., Li, S., 2024. Optimal three-dimensional particle shapes for maximally dense saturated packing. *J. Chem. Phys.* 161, 014505.

Radovitzky, R., Ortiz, M., 2000. Tetrahedral mesh generation based on node insertion in crystal lattice arrangements and advancing-front-delaunay triangulation. *Computer Methods in Applied Mechanics and Engineering* 187, 3-4, 543–569.

Romanova, T., Bennell, J., Stoyan, Y., Pankratov, A., 2018. Packing of concave polyhedra with continuous rotations using nonlinear optimisation. *European Journal of Operational Research* 268, 1, 37–53.

Romanova, T., Stoyan, Y., Pankratov, A., Litvinchev, I., Kravchenko, O., Duryagina, Z., Melashenko, O., Chugai, A., 2023. Optimized packing soft ellipses. In *Human-Assisted Intelligent Computing: Modeling, simulations and applications*. booktitle, pp. 9.1–9.14.

Romanova, T., Stoyan, Y., Pankratov, A., Litvinchev, I., Marmolejo, J., 2020. Decomposition algorithm for irregular placement problems. In Vasant, P., Zelinka, I. and Weber, G. (eds), *Intelligent Computing and Optimization. ICO 2019*, *Advances in Intelligent Systems and Computing*. Vol. 1072. Springer, Cham, pp. 214–221.

Scheithauer, G., 2018. *Introduction to Cutting and Packing Optimization. Problems, Modeling Approaches, Solution Methods*. Springer International Series in Operations Research & Management Science. Springer.

Schwartz, J., 1954. The formula for change in variables in a multiple integral. *The American Mathematical Monthly* 61, 2, 81–85.

Stoyan, Y., Pankratov, A., Romanova, T., 2016. Quasi-phi-functions and optimal packing of ellipses. *Journal of Global Optimization* 65, 2, 283–307.

Tawarmalani, M., Sahinidis, N.V., 2005. A polyhedral branch-and-cut approach to global optimization. *Mathematical Programming* 103, 2, 225–249.

Tollenaere, J., Sykora, T., Wauters, T., 2025. Mixed-integer linear programming models for 3D irregular strip packing problems. *European Journal of Operational Research*. doi: 10.1016/j.ejor.2025.10.041.

Wachter, A., Biegler, L., 2006. On the implementation of an interior-point filter line-search algorithm for large-scale nonlinear programming. *Mathematical Programming* 106, 1, 25–57.

Wang, C., Yao, Y., Huang, Z., Liu, F., Yang, Y., 2024. Digital core reconstruction based on discrete element and markov chain-monte carlo methods. *Geoenergy Science and Engineering* 236, 212422.

Wäscher, G., Haußner, H., Schumann, H., 2007. An improved typology of cutting and packing problems. *European Journal of Operational Research* 183, 1109–1130.

Winkelmann, J., Chan, H., 2023. *Columnar structures of spheres: Fundamentals and applications*. Jenny Stanford Publishing, NY.

Xie, Z., An, X., Wu, Y., Wang, L., Qian, Q., Yang, Y., 2017. Experimental study on the packing of cubic particles under three-dimensional vibration. *Powder Technology* 317, 13–22.

Yuan, Q., Li, Z., Gao, Y., Wang, Y., Li, X., 2019. Local responses in 2d assemblies of elliptical rods when subjected to biaxial shearing. *Acta Geotech* 14, 1685–1697.

Zhang, H., 2004. Packing: scheduling, embedding, and approximating metrics. In Lagana, A., Gavrilova, M.L., Kumar, V.,

Mun, Y., Tan, C.J. and Gervasi, O. (eds), *Computational Science and Its Applications – ICCSA*. Springer, Berlin, pp. 764–775.

Zhang, T., Xia, P., Lu, F., 2021. 3d reconstruction of digital cores based on a model using generative adversarial networks and variational auto-encoders. *Journal of Petroleum Science and Engineering* 207, 109151.

Zhao, B., An, X., Wang, Y., Zhao, H., Shen, L., Sun, X., Zou, R., 2020a. Packing of different shaped tetrahedral particles: Dem simulation and experimental study. *Powder Technology* 360, 21–32.

Zhao, B., An, X., Zhao, H., Gou, D., Shen, L., Sun, X., 2020b. Dem simulation on random packings of binary tetrahedron-sphere mixtures. *Powder Technology* 361, 160–170.

Zhao, S., Zhou, X., Liu, W., Lai, C., 2015. Random packing of tetrahedral particles using the polyhedral discrete element method. *Particuology* 23, 109–117.

Zuo, Q., Liu, X., Xu, L., Xiao, L., Xu, C., Liu, J., Chan, W., 2022. The three-dimensional bin packing problem for deformable items. In *2022 IEEE International Conference on Industrial Engineering and Engineering Management (IEEM)*, pp. 0911–0918.

Appendix A. Basic phi-function definitions

To place feasibly two objects within a container, an analytical description of the relations between the pair of objects is required. In this paper the phi-function technique is used to express this relation. Let A and B be three-dimensional objects. The position of the object A is defined by a vector of placement parameters $u_A = (v_A, \theta_A)$, where: $v_A = (x_A, y_A, z_A)$ is a translation vector and θ_A is a vector of rotation parametrs. The object A, rotated by θ_A and translated by v_A is denoted by $A(u_A)$.

A continuous function $\Phi^{AB}(u_A, u_B)$ is called a phi-function of the objects $A(u_A)$ and $B(u_B)$ if the following conditions are fulfilled (Chernov et al. (2010)):

- $\Phi^{AB}(u_A, u_B) > 0$, for $A(u_A) \cap B(u_B) = \emptyset$;
- $\Phi^{AB}(u_A, u_B) = 0$, for $intA(u_A) \cap intB(u_B) = \emptyset$ and $frA(u_A) \cap frB(u_B) \neq \emptyset$;
- $\Phi^{AB}(u_A, u_B) < 0$, for $intA(u_A) \cap intB(u_B) \neq \emptyset$.

Here frA denotes the boundary (frontier) of the object A, while $intA$ stands for its interior.

Thus, $\Phi^{AB}(u_A, u_B) \geq 0 \Leftrightarrow intA(u_A) \cap intB(u_B) = \emptyset$.

Note, that the phi-function $\Phi^{AB}(u_A, u_B)$ for a pair of objects A and B can be constructed in different ways, and the most convenient representation can be used in designing optimization algorithms.

Now define a function $\Phi'^{AB}(u_A, u_B, \tau_{AB})$ introducing auxiliary variables τ_{AB} defined in a domain $U \subset R^n$ depending on the shapes of the objects A and B. This function is defined for all values of u_A, u_B and has to be continuous in all its variables.

By the definition ((Stoyan et al. (2016)), the function $\Phi'^{AB}(u_A, u_B, \tau_{AB})$ is called a quasi-phi-function for two objects $A(u_A)$ and $B(u_B)$ if $\max\limits_{\tau_{AB} \in U} \Phi'^{AB}(u_A, u_B, \tau_{AB})$ is a phi-function for the objects.

The definition of the quasi-phi-function provides an additional "degree of freedom" since the auxiliary variables τ_{AB} can be chosen as necessary.

The general property of the quasi-phi-function for two objects $A(u_A)$ and $B(u_B)$ is as follows: if $\Phi'^{AB}(u_A, u_B, \tau_{AB}) \geq 0$ for some τ_{AB}, then $intA(u_A) \cap intB(u_B) = \emptyset$.

Appendix B. Table of Notations

Table B1

n	the number of convex polyhedra
$I_n = \{1, 2, ..., n\}$	index set
$P_i,\ i \in I_n$	set of convex polyhedra
m_i	the number of vertices of P_i
$J_i = \{1, 2, ..., m_i\}$	index set
$\tilde{X}_i^k = (\tilde{x}_i^k, \tilde{y}_i^k, \tilde{z}_i^k),\ k \in J_i$	vertices of polyhedron P_i
$\Omega(L) \subset \mathbb{R}^3$	convex bounded region (container)
$L \in \mathbb{R}^\sigma$	vector of variable metric characteristics of Ω
σ	the number of variable metric characteristics of Ω
$v_i = (x_i, y_i, z_i)$	translation vector of P_i
$\theta_i = (\theta_i^1, \theta_i^2, \theta_i^3)$	vector of rotation parameters of P_i
$u_i = (v_i, \theta_i)$	vector of placement parameters of P_i
$\mu_i = (\mu_i^x, \mu_i^y, \mu_i^z)$	vector of deformation parameters of P_i
μ_x^-, μ_x^+	given deformation limits of μ_i^x
μ_y^-, μ_y^+	given deformation limits of μ_i^y
μ_z^-, μ_z^+	given deformation limits of μ_i^z
$A(\mu_i)$	deformation matrix
$M(\theta_i)$	rotation matrix
$\Lambda = \{(i, j) \in I_n \times I_n : i < j\}$	index set of pairs of polyhedra
$\tau_{ij}, (i, j) \in \Lambda$	vector of additional variables of quasi-phi-functions φ_{ij}
$\varphi_{ij}(u_i, u_j, \mu_i, \mu_j, \tau_{ij})$	quasi-phi-function for non-overlapping of soft polyhedra $P_i(u_i, \mu_i)$ and $P_j(u_j, \mu_j)$
$\psi_i(u_i, \mu_i, L)$	phi-function for containment polyhedron $P_i(u_i, \mu_i)$ into container $\Omega(L)$
$\kappa(L)$	objective function
λ	scaling parameter of each sphere $S_i,\ i \in I_n$ in Algorithm 1
$\delta = \mu^+ \cdot \max\limits_{i \in I_n} r_i$	decomposition parameter in Algorithm 2
ε	computational accuracy in Algorithm 2
Δ	parameter of the border-wall effect in the case study